

# THE CONCEPT OF A MECHANISM FOR THE FORMATION OF BIMETALLIC STRUCTURES

MILAN SAGA<sup>1</sup>, VYACHESLAV B. DEMENTYEV<sup>2</sup>,  
ALEKSANDR I. KORSHUNOV<sup>2</sup>, MILAN VASKO<sup>1</sup>,  
VLADIMIR P. KORETSKII<sup>3</sup>, PAVOL BOZEK<sup>1</sup>

<sup>1</sup>University of Zilina, Faculty of Mechanical Engineering,  
Zilina, Slovak Republic

<sup>2</sup>Udmurt Federal Research Center of the Ural Branch of  
the RAS, Institute of Mechanics, Izhevsk, Udmurt Republic

<sup>3</sup>MIREA, RTU, Moscow, RF

DOI: 10.17973/MMSJ.2025\_10\_2025079

pavol.bozek@fstroj.uniza.sk

The paper describes an approach to the activation energy and diffusivity calculation concept for the formation of bimetallic structures, which is based on the interatomic potential idea. A comparative analysis of the computed values obtained with the proposed model and the real data for a range of metals has been carried out, which demonstrates and confirms the accuracy and validity of the model, which needs further refinement. This is not inconsistent with the justification of the possibility of using this method, with certain assumptions, to deal with theoretical issues in the field of development and analysis of the interaction of elements, structure, and parameters of bimetallic materials. The proposed model does not contradict the available experimental data and provides some promise for its further development and improvement.

## KEYWORDS

Activation energy, Diffusivity coefficient, Bimetallic alloys, Interatomic potential

## 1 INTRODUCTION

Since the first mathematical models of neurons [McCulloch 1943], artificial neural networks have come a long way in development, becoming the foundation of artificial intelligence. Modern ANNs demonstrate exceptional efficiency in highly specialized tasks (pattern recognition, natural language processing). However, despite impressive practical successes, a fundamental gap remains between biological reality and its computational models. The successes of ANNs are based on statistical patterns, not on the reproduction of the principles of biological brain operation. The gap between ANNs and biological neural networks (BNNs) manifests itself in three key aspects: a simplified view of neural signal transmission and processing; ignoring the spatio-temporal organization of neural ensembles; and the lack of genuine mechanisms of self-organization and adaptation. In this paper, we formulate an alternative approach to modeling neural-like networks. We conduct a systematic analysis of the limitations of existing generations of ANNs, justify the necessity of considering biological principles, propose a new architecture based on self-organizing networks of uniform elements (SNUE), and define promising research directions. In accordance with the concepts prevailing in the scientific community, the atomic interaction takes place by Coulomb interaction between their nuclei and electron shells [Baranov 1998, Kittel 2005]. With that knowledge in mind, assuming that the inner shells of atoms

shield the nucleus, and the interaction between atoms in the crystalline state is mainly due to the outermost shells, whose density is many times less than the inner ones, the influence of quantum effects in the interatomic interaction is insignificant [Baranov 1984, Miglierini 2004 & 2006, Naumov 2012]. Having assumed that the electron configurations of atoms are known, the potential energy of their interaction (the so-called interatomic potential) can be defined as the Coulomb interaction between atomic nuclei and shells. Consequently, the basic elements are not indispensable for the configuration of the outermost electron shells to be determined. Assuming that the form of the electron density distribution function in an atom is known, the parameters of this distribution are enough to define the experimental characteristics of single-component crystals, in particular, metals as a base [Vol 1962]. These parameters can be defined by solving the appropriately casted inverse problem of electrostatics and should, accordingly, show themselves in the expression for the interatomic potential, if one can be found. This point is essential, since with a known electron density distribution in an atom, it becomes possible to describe multicomponent systems. By modifying the kind of this distribution, it is possible to ensure that the calculated values of the known crystal characteristics are sufficiently close to the experimental ones. In this case, the type of electron distribution can be assumed to be approximately the same as real atoms.

## 2 MATERIAL AND METHODS

The potential of the electrostatic interaction between atoms unambiguously depends on the nature of the electron density distribution in the atomic shells. In the proposed model, the electron density of atoms is defined as the density of the inner and outermost shells [Orlov 1983]. The density of inner shells can be considered localized near the nucleus in such a way that their overlap with the electron density of neighboring atoms can be disregarded.

We assume that  $q_1$  the charge of the outermost shells is evenly distributed on the surface of a thin sphere of radius  $R_1$  centered on the atomic center, and it is compensated by a part of the charge of the nucleus that is not compensated by the charge of the inner shells.

Let us see in detail about the interaction between atoms 1 and 2 with the parameters of the distributions ( $R_1, q_1$ ) and ( $R_2, q_2$ ), respectively. Let  $R$  be the distance between the centers of the atoms (Figure 1).

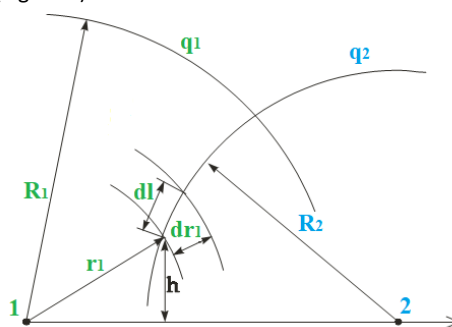


Figure 1. Diagram of the overlap of the electron shells of atoms 1 and 2

In accordance with the above, the interaction between atoms is caused only by electrostatic forces; in this case, the potential of interatomic interaction can be represented in the following form:

$$\phi(R) = \phi_{c_1-c_2}(R) + \phi_{c_1-n_2}(R) + \phi_{n_1-c_2}(R) + \phi_{n_1-n_2}(R) \quad (1)$$

Where the first term is responsible for the interaction between the electron shells of atoms 1 and 2, the second and third

terms, respectively, correspond to the interaction between shells and nuclei, respectively, and the last term refers to the interaction between nuclei.

Generally, each of the terms (formula 1) can be found by the integration of the Coulomb interaction energy density of the corresponding electronic distributions.

The energy of interaction between nuclei is the simplest to be determined:

$$\phi_{n_1-n_2}(R) = k \frac{q_1 q_2}{R} \quad (2)$$

where  $k$  is the coefficient that depends on the unit amount system. In particle physics, the charge is usually measured in elementary electric charges  $e$ , the distance, respectively, in angstroms, and the energy in electron volts [Gulyaev 2022]. Having this choice, the coefficient can be written as follows:

$$k = 14,4 (eV \cdot \text{\AA})/e^2 \quad (3)$$

Denoting the potential of the outermost electron shells of atom 1 at a distance  $r$  from the nucleus by  $\Phi_1(r)$ , and by  $\Phi_2(r)$  the corresponding potential of the outermost electron shells of atom, we have:

$$\Phi_1(r) = \begin{cases} k \frac{q_1}{R_1}, & r < R_1 \\ k \frac{q_1}{r}, & r \geq R_1 \end{cases} \quad (4)$$

The potential  $\Phi_2(r)$  has the same form.

In this case, the energies of interaction between charged spheres and the nuclei of neighboring atoms have been written as follows:

$$\phi_{c_1} - \phi_{c_2} = \Phi_1(R) \cdot q_2 = \begin{cases} -k \frac{q_1 q_2}{R_1}, & R < R_1 \\ -k \frac{q_1 q_2}{R}, & R \geq R_1 \end{cases} \quad (5)$$

$$\phi_{c_2-n_1} = \Phi_2(R) \cdot q_1 = \begin{cases} -k \frac{q_1 q_2}{R_2}, & R < R_2 \\ -k \frac{q_1 q_2}{R}, & R \geq R_2 \end{cases} \quad (6)$$

Next, the interaction between the shells of atom 1 and atom 2 needs to be considered. Obviously, when the electron shells do not overlap at large interatomic distances, the interaction between shells takes the following form:

$$\phi_{c_1-c_2} = k \frac{q_1 q_2}{R} \quad (7)$$

which, in fact, corresponds to the energy of the interaction between the nuclei (2).

In the case of overlapping electron shells of atoms, the overlap condition can be represented as an inequality  $R < R_1 + R_2$ .

Let us define the radius vector  $\vec{r}_1$  with the tail located at the center of the nucleus of atom 1 and the head at the electron shell point of atom 2, near which the charge  $dq_2$  is located; that is one of the points of sphere 2. Then the interaction between shells takes the following form:

$$\phi_{c_1-c_2} = \int_{\text{by sphere 2}} \Phi_1(r) dq_2 \quad (8)$$

The charge  $dq_2$  (formula 8) refers to a certain part of the charge of the shell of the atom 2 located on a thin ring of radius  $h$  and width  $dl$  (Figure 1). The distance from any point of this ring to the corresponding nuclei remains unchanged. Accordingly

$$dq_2 = \frac{q_2}{4\pi R_2^2} 2\pi h dl = k \frac{q_2}{2RR_2} r_1 dr_1 \quad (9)$$

The potential  $\phi_{c_1-c_2}$  should be represented as two integrals, in the first of which integration runs over the area of sphere 2

located inside the sphere with radius  $R_1$ , and in the second over the remaining part of sphere 2:

$$\phi_{c_1} - \phi_{c_2} = k \frac{q_1 q_2}{2RR_2} \int_{|R-R_2|}^{R_1} \frac{r_1}{R_1} dr_1 + \int_{R_1}^{R+R_2} k \frac{q_1 q_2}{2RR_2} dr_1 \quad (10)$$

The integration results look like this

$$\phi_{c_1} - \phi_{c_2} = k \frac{q_1 q_2}{2} \left[ \frac{1}{R} + \frac{1}{R_1} + \frac{1}{R_2} - \frac{R^2 + R_1^2 + R_2^2}{2RR_1R_2} \right] \quad (11)$$

For definiteness, let us assume that  $R_1 > R_2$ . In this case, after combining expressions (2), (5), (6) and (11), the formula (1) for the interatomic potential can be written as a piecewise smooth function:

$$\phi(R) = \begin{cases} k \frac{q_1 q_2}{2} \left[ \frac{3}{R} - \frac{1}{R_1} - \frac{1}{R_2} - \frac{R^2 + R_1^2 + R_2^2}{2RR_1R_2} \right], & \text{when } R \leq R_2 \\ k \frac{q_1 q_2}{2} \left[ \frac{1}{R} - \frac{1}{R_1} + \frac{1}{R_2} - \frac{R^2 + R_1^2 + R_2^2}{2RR_1R_2} \right], & \text{when } R_2 < R \leq R_1 \\ k \frac{q_1 q_2}{2} \left[ -\frac{1}{R} + \frac{1}{R_1} + \frac{1}{R_2} - \frac{R^2 + R_1^2 + R_2^2}{2RR_1R_2} \right], & \text{when } R_1 < R \leq R_1 + R_2 \\ 0, & \text{for } R > R_1 + R_2 \end{cases} \quad (12)$$

Assuming that the interacting atoms are the identical, i.e.,  $q_1 = q_2$ , and  $R_1 = R_2$ , after the suitable transformations, the expression for the interatomic potential significantly simplifies to the following expression:

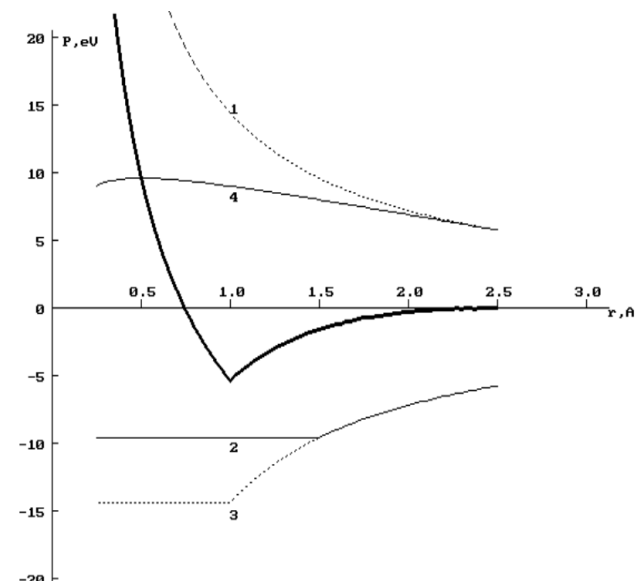
$$\phi(R) = \begin{cases} k q_1^2 \left[ \frac{1}{R} - \frac{1}{R_1} - \frac{R}{4R_1^2} \right], & 0 < R \leq R_1 \\ k q_1^2 \left[ \frac{1}{R_1} - \frac{1}{R} - \frac{R}{4R_1^2} \right], & R_1 < R \leq 2R_1 \\ 0, & \text{for } R \geq 2R_1 \end{cases} \quad (13)$$

Figure 2 shows the type of interatomic potential (121) and its components. The analysis of the graph shows that the interatomic potential is a piecewise smooth function with singular points  $R = R_1$  and  $R = R_2$ .

The internal energy of a single-component crystal is represented as the sum of the energies of paired interatomic interactions:

$$U(a) = \frac{1}{2} \sum_j \phi(r_j) \quad (14)$$

where  $\phi(r_j)$  has the form of the expression (14),  $a$  is a lattice constant.



**Figure 2.** Type of interatomic potential (11) (thickened line) and its components. ( $q_1=1$ ,  $R_1= 1,5 \text{ \AA}$ ), ( $q_1=1$ ,  $R_1= 1,0 \text{ \AA}$ ) where: 1 - ( $\phi_{n_1} - \phi_{n_2}$ ), 2 - ( $\phi_{n_2} - \phi_{c_1}$ ), 3 - ( $\phi_{n_1} - \phi_{c_2}$ ), 4 - ( $\phi_{c_1} - \phi_{c_2}$ )

For definiteness, decided  $\frac{R_1}{a_0} = 1$ . Then, calculated using the formula (14) the dependence  $U(a)$  for elements with a face-centered cubic (FCC) lattice has the form shown in Figure 3.

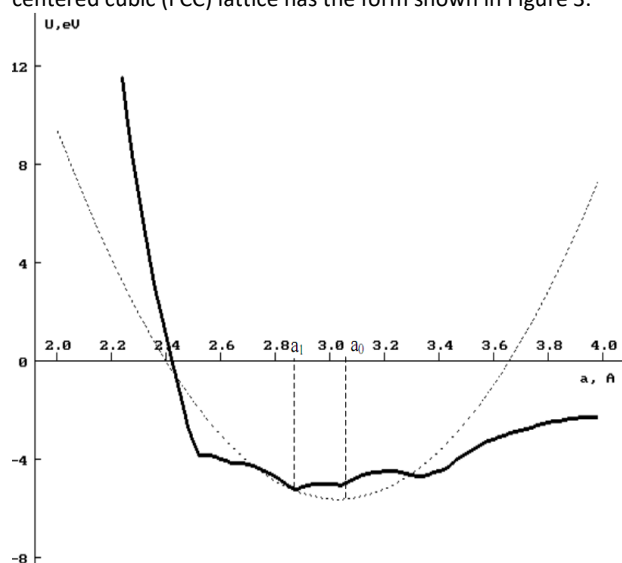


**Figure 3.** The dependence of the internal energy of an element with an FCC lattice on a lattice constant ( $a$ ) and the scheme for determining the equilibrium value of the lattice constant

### 3 RESULTS AND DISCUSSION

Analysis of the graph develops a conviction that the dependence of the internal energy on the lattice constant is also a piecewise smooth function. The presence of piecewise smoothness intervals is due to the fact that the lattice constant of an increasing number of spheres falls within the range of the potential ( $R < R_1 + R_2$ ).

Formally, condition (15) can be met at several points in particular, at the singular points of the curve. However, these values of lattice constant are not acceptable in terms of physics. An identical functional connection  $U(a)$  is obtained with another choice  $R_1$ . In view of these circumstances, it becomes obvious that the derivative  $\frac{dU}{da}$  must be determined using numerical techniques, in particular mesh schemes. In this case, the differentiation step  $\Delta a$  should be chosen large enough to cover several smooth intervals (Figure 3).

Let us determine the trial value of the lattice constant  $a_1$  in the vicinity of the expected one for a sufficiently large interval  $\Delta a$ . The values of the internal energy at points  $a_1 - \Delta a$ ,  $a_1$ ,  $a_1 + \Delta a$  are denoted, respectively, as  $U_1$ ,  $U_2$ ,  $U_3$ ; that is  $U_1 = U(a_1 - \Delta a)$ ,  $U_2 = U(a_1)$ ,  $U_3 = U(a_1 + \Delta a)$ . These three points determine a parabola. The position of the minimum of this 2-degree polynomial indicates the equilibrium value of the lattice constant  $a_0$ . The value of the minimum energy on the parabola must correspond to the value of the sublimation energy  $E_s$ . By successive varying the value  $R_1$ , it can be chosen in such a way that the found using the above-described schemes value of the lattice constant corresponds to the experimental value  $a_0$ .

The value of the shell charge is chosen from the condition (14), taking into account the parabola minimum's depth.

The diagram above shows that the values  $R_1$  are determined only by the type of crystal lattice and the value  $a_0$ . Therefore,

for metals with the same type of crystal lattice, the ratio  $\frac{R_1}{a_0}$  should remain unchanged. Indeed, calculations show that for

metals with a FCC lattice the ratio  $\frac{R_1}{a_0}$  is equal to 0.75007. This means that the interatomic interaction is nonzero only for

atoms located at the distance of the first coordination shells. Moreover, the atoms located at the distance of the first coordination shell ( $r_1 = 0.707a_0 < R_1$ ) are repelled from each other. In contrast, atoms located in the nodes of the second or fourth shells have mutual attraction.

A slightly different picture is for crystals with a body-centered

cubic (BCC) lattice, where  $\frac{R_1}{a_0} = 1.00249$ . The potential in the BCC lattice consists of six spheres. Moreover, the first two shells demonstrate "repulsion", and the third to the sixth, respectively, realize "attraction".

The absolute value  $R_1$  and charge value, expressed in elementary charges, found according to the above scheme for most elements with a FCC and BCC lattice, together with the initial experimental values of the lattice parameter and the sublimation energy, are shown in Table 1.

**Table 1.** Initial experimental data and calculated values of parameters  $R_1$  and  $q_1$  for some elements [Baranov 2017]

Element	Initial experimental data			Calculated Value	
	Lattice Type	$a_0$ , Å	$E_s$ , eV	$R_1$ , Å	$q_1/e$
Li, Lithium	BCC	3.509	1.650	3.5177	0.5014
Na, Natrium	BCC	4.291	1.130	4.3017	0.4589
K, Kalium	BCC	5.247	0.941	5.2601	0.4630
Rb, Rubidium	BCC	5.700	0.858	5.7142	0.4608
Cs, Cesium	BCC	6.140	0.827	6.1523	0.4696
V, vanadium	BCC	3.028	5.300	3.0355	0.8348
Cr, Chromium	BCC	2.885	4.100	2.8922	0.7167
Fe, Ferrum	BCC	2.866	4.290	2.8731	0.7307
Nb, Niobium	BCC	3.301	7.470	3.3092	1.5566
Mo, Molybdenum	BCC	3.147	6.810	3.1548	0.9647
Ba, Barium	BCC	5.025	1.860	5.0375	0.6371
W, Wolfram	BCC	3.165	8.660	3.1729	1.0909
Eu, Europium	BCC	4.606	1.800	4.6175	0.6000
Ta, Tantalum	BCC	3.805	8.089	3.8145	1.1561
Pa, Protactinium	BCC	3.925	5.460	3.9348	0.9647
Ne, Neon	FCC	4.430	0.020	3.3228	0.0544
Ar, Argon	FCC	5.260	0.080	3.9454	0.1186
Kr, Krypton	FCC	5.720	0.116	4.2979	0.1491
Al, Aluminium	FCC	4.049	3.340	3.0370	0.6725
Ca, Calcium	FCC	5.582	1.825	4.1869	0.5836
Ni, Nickel	FCC	3.524	4.435	2.6432	0.7229
Cu, Cuprum	FCC	3.615	3.500	2.7115	0.6504
Rh, Rhodium	FCC	3.803	5.752	2.8525	0.8552
Pd, Palladium	FCC	3.889	3.936	2.9170	0.7154
Ag, Argentum	FCC	4.086	2.960	3.0648	0.6359
Ir, Iridium	FCC	3.839	6.930	2.8795	0.9432
Pt, Platinum	FCC	3.923	5.852	2.9425	0.8762
Au, Aurum	FCC	4.079	3.780	3.0595	0.7180
Ce, Cerium	FCC	5.161	4.770	3.8711	0.9073
Pr, Praseodymium	FCC	5.160	3.900	3.8704	0.8203
Yb, Ytterbium	FCC	5.486	1.600	4.1149	0.5418
Pb, Plumbum	FCC	5.084	5.926	3.8134	1.0037

It should be noted that the values  $R_1$  of and  $q_1$  given in Table 1, are not the only solutions obtained in accordance with above-described algorithm. For example, an alternative solution for Fe can be  $R_1/a_0=2,07$  and  $q_1=0,762$ . However, such solution means that atoms located at a distance of up to the 12th coordination shell should interact, which seems implausible.

The internal energy of an ordered alloy per structural unit is calculated from the relation:

$$U_{\text{alloy}}(a) = \frac{1}{2} \sum_m \sum_n \phi_{mn}(r_{mn}) \quad (14)$$

Here:

the index  $m$  denotes the number and type of an atom in the structural unit of the superstructure under consideration (for example,  $\text{Fe}_1$ ,  $\text{Fe}_2$ ,  $\text{Fe}_3$ ,  $\text{Al}_1$  in the structural unit  $\text{Fe}_3\text{Al}$  of the corresponding alloy with the superstructure  $\text{DO}_3$ ;

$n$  – the number and type of an atom from the  $m$ th atom circumference within the considered number of coordination shells;

$r_{mn}$  is the interatomic distance proportional to the lattice constant  $a$  of the alloy.

The equilibrium value  $a_0$  of the lattice constant is determined from the minimum condition of the function  $U_{\text{alloy}}$  approximating the internal energy of the alloy by a parabola:

$$\frac{d\tilde{U}_{\text{alloy}}}{da} = 0 \quad (15)$$

The cohesive energy of the alloy  $E_{\text{cohesive}}$  was taken as the value of its internal energy found for the equilibrium lattice constant:

$$E_{\text{cohesive}} = U(a). \quad (16)$$

The values of the cohesive energy of binary alloys found from (16) were compared with a value  $H$  that could fairly be named the “proper contribution” to the cohesive energy.

$$H = n_A E_{sA} + n_B E_{sB}, \quad (17)$$

where  $n_A$  and  $n_B$  are the numbers of atoms of the class  $A$  and  $B$  in the structural unit of the element.

The experimental value of the cohesive energy differs from  $H$  by the value of the heat of mixture  $\Delta H$ :

$$E_{\text{coh.exp}} = H + \Delta H \quad (18)$$

The values of lattice constants, cohesive energies, and the corresponding observed values [Hansen 1962, Elliot 1970, Gorelik 1970] of alloys ordered into superstructures  $B_2$ ,  $\text{DO}_3$ ,  $L_{12}$ , are calculated in accordance with the described algorithm, and shown in Table 2. Due to the parabolic approximation of the internal energy there is some arbitrariness for the calculated values  $a_0$ ,  $E_{\text{cohesive}}$  presented in Table 2. In fact, these numbers depend not only on the type of function  $U(a)$ , but also on the initial value  $a_1$  and the stride parameter  $\Delta a$  (Figure 3). During the calculation, the value  $a_1$  was set as an integer number of angstroms, the closest to the observed value. Trial step  $\Delta a$  was  $0,2 \cdot a_1$ .

Table 2 shows that in alloys with a superstructure  $B_2$ , the calculated values of the lattice constants are less than the observed values. Exceptions are the alloys  $\text{AlFe}$  and  $\text{AlPd}$ , for which constants  $a_{\text{calc}}$  almost coincide with the experimental value. For some alloys ( $\text{AgPr}$ ,  $\text{AuCs}$ ,  $\text{NaAl}$ ), the decrease is quite significant (up to 25% in  $\text{AuCs}$ ). This is explained by the difference in the parameters of the atomic shells of the components ( $q_1$ ,  $R_1$  and  $q_2$ ,  $R_2$ ) and, as a result, by the large number of singularities in the graph  $U_{\text{alloy}}(a)$ . In alloys with superstructures  $\text{DO}_3$ ,  $L_{12}$  deviations  $a_{\text{calc}}$  from  $a_{\text{exp}}$  can be either positive or negative.

The expected values of the cohesive energies of alloys should be greater by modulus than the value  $H$  given in Table 2, due to the formation of a stable compound and the heat of mixing emission. However, this inequality does not hold in most cases. So, in the superstructure  $B_2$  it is valid only for alloys  $\text{AlPd}$ ,  $\text{CuPd}$  and  $\text{NaAl}$ . However, the differences between  $E_{\text{cohesive}}$  and  $H$  in these alloys are insignificant. In superstructures  $\text{DO}_3$ , the  $L_{12}$  “right” proportion between these values is observed for about half of the alloys.

Thuswise, within the framework of the developed concept based on the action of Coulomb forces only, both at the stage of constructing electronic distributions in atoms and at the stage of their application, and assuming that the electronic shells of atoms are given in the form of thin spheres, the parameters of the corresponding electronic distributions are determined.

**Table 2.** Equilibrium calculated and observed characteristics of some binary alloys with superstructures  $B_2$ ,  $\text{DO}_3$ ,  $L_{12}$

Superstructure	Alloy	$a_0(\text{\AA})$ calculated	$a_0(\text{\AA})$ observed	$E_{\text{cohesive}}$ , Ev Calculation	$H$ , Ev
<b>B2</b>	AgCe	3.718	3.740	7.235	7.730
	AgLi	3.003	3.174	4.249	4.610
	AgPr	3.458	3.735-3.739	6.551	6.860
	AlFe	2.987	2.900	7.448	7.630
	AlIr	2.925	2.977	9.864	10.270
	AlNi	2.809	2.887	7.201	7.775
	AlPd	3.096	3.030	7.286	7.276
	AlPr	3.514	3.820	6.998	7.240
	AlRh	2.933	2.990	8.751	9.092
	AuCs	3.360	4.263	3.677	4.607
	AuPr	3.386	3.680	7.118	7.680
	CuPd	2.883	2.994	7.489	7.436
	FeRh	2.915	2.987	10.043	10.042
	NaAl	3.037	3.730	4.505	4.470
<b>DO3</b>	AlCu <sub>2</sub>	5.843	5.900	13.500	13.840
	AlFe <sub>3</sub>	6.032	5.780	15.823	16.210
	AlCe <sub>3</sub>	4.932	4.985-5.013	14.884	17.650
	AlNi <sub>3</sub>	3.975	3.560	15.123	16.645
<b>L13</b>	AlPr <sub>3</sub>	5.453	4.950-5.007	14.295	15.040
	AlPt <sub>3</sub>	4.374	3.876	19.981	20.896
	Cu <sub>3</sub> P	3.821	3.650	15.927	14.436
	Cu <sub>3</sub> Al	3.797	3.750	15.283	14.280
	Cu <sub>3</sub> P	3.809	3.68	17.566	16.352
	FePd	3.899	3.848-3.851	16.298	16.098
	Ir <sub>3</sub> Ta	3.822	3.861-3.889	29.383	28.879
	Ir <sub>3</sub> V	3.897	3.812	3.812	26.090
	NbRh	3.815	3.865	31.309	24.726
	Pt <sub>3</sub> V	3.892	3.870	21.898	22.856
	Pt <sub>3</sub> Zn	3.869	3.890	18.343	18.906
	Rh <sub>3</sub> Si	3.938	3.900	21.477	21.256
	Rh <sub>3</sub> T	4.034	3.860	25.794	25.345
	Rh <sub>3</sub> T	3.829	4.139	24.094	23.182

Potentials describing the interaction of various types of atoms have been constructed, the most important characteristics of metal crystals and binary alloys have been calculated, and a comparison has been made with the available observed data. It is also worthy of note that in general, due to the piecewise smoothness of the constructed interatomic potentials and the lattice constant dependence of the internal energy, the proposed model fails to describe the properties of metals and alloys well adequately, and the proposed model requires further refinement. Nevertheless, the calculations show that the necessary conditions for the stability of the crystal lattice can be met if the electron density of the outermost shells is represented as a function, "blurred" near the surface of a sphere of a certain radius  $R_1$ .

#### 4 CONCLUSIONS

To enable an adequate description of the physicochemical processes involved in the formation of bimetals, a method for determining the interaction potentials between different types of atoms included in a particular test compound has been proposed. The method is based on the electrostatic nature of the interaction between the outermost electron shells of atoms. The effect of other factors is seen as insignificant. Comparing the experimental values of the crystal lattice size and binding energy of single and binary compounds with the calculated ones led to the conclusion that they correspond in the presence of certain deviations that are systemic in nature, which indicates the need for further improvement of the proposed model. Based on this, the conclusion about the principal possibility of using the proposed model interaction potential in the study of interatomic kinetics of bimetals has been drawn.

#### ACKNOWLEDGMENTS

This work is supported by VEGA project No. 1/0423/23 Experimental research and simulation of dynamic properties of composite structural elements manufactured by 3D printing.

#### REFERENCES

[Baranov 1984] Baranov, M.A., Starostenkov, M.D. Calculation of the equilibrium properties of metal systems in

the semiclassical approximation. VINITI Department, 1984, No. 3712-84, 31 p.

[Baranov 1998] Baranov, M.A., Starostenkov, M.D. Quasi-electrostatic approach to the description of metal systems. AltSTU, Barnaul, 1998, 40 p.

[Baranov 2017] Baranov, M.A. The correlation of properties of crystals and the distribution of peripheral electrons in the shells of forming them atoms. Symbol of Science, 2017, No. 2, pp. 15-21.

[Elliot 1970] Elliot, R.P. Structures of binary alloys. M.I. Novikov and I.L. Ryelberga (Eds). Metallurgiya, Moscow, 1970.

[Gorelik 1970] Gorelik, S.S., Rastorguev, L.N., Skakov, Yu.A. X-ray and electron-optical analysis. Metallurgiya, Moscow, 1970, 107 p.

[Gulyaev 2022] Gulyaev, P., et al. Particle and Particle Agglomerate Size Monitoring by Scanning Probe Microscope. Applied Sciences, 2022, Vol. 12, No. 4. DOI: 10.3390/app12042183.

[Hansen 1962] Hansen, M., Andreko, K. Structural properties of binary alloys. Metallurgiya, Moscow, 1962.

[Kittel 2005] Kittel, C. Introduction to solid state physics, 8<sup>th</sup> ed. Wiley, New York, 2005, 680 p. ISBN 978-0-471-68057-4.

[Miglierini 2004] Miglierini, M., Kanuch, T., Krenicky, T., Skorvanek, I. Magnetic and Mossbauer studies of Fe<sub>76</sub>Mo<sub>8</sub>Cu<sub>1</sub>B<sub>15</sub> nanocrystalline alloy. Czechoslovak J. of Physics, 2004, Vol. 54, pp. 73-76.

[Miglierini 2006] Miglierini, M., et al. Magnetic microstructure of NANOPERM-type nanocrystalline alloys. Physica Status Solidi (B), 2006, Vol. 243, Issue 1, pp. 57-64. DOI: 10.1002/PSSB.200562446.

[Naumov 2012] Naumov, V.I., Panicheva, G.A., Chetyrebok, L.N., Matsulevich, Zh.V. Chemical bond and structure of matter. NNSTU, R.E. Alekseev, Nizhny Novgorod, 2012, 344 p. (in Russian)

[Orlov 1983] Orlov, A.N., Trushin, Yu.V. Energy of point imperfection. Energoatomizdat, Moscow. 1983, 82 p.

[Vol 1962] Vol, A.E. Structure and properties of binary metal systems. Fizmatgiz, Moscow, 1962.

#### CONTACTS:

**Milan Saga**, Dr.h.c., Prof. Dr. Ing. University of Zilina, Faculty of Mechanical Engineering, Zilina, Slovak Republic  
e-mail: [milan.saga@fstroj.uniza.sk](mailto:milan.saga@fstroj.uniza.sk)

**Vyacheslav B. Dementyev**, Doctor of Technical Sciences, Professor, Chief Researcher  
**Aleksandr I. Korshunov**, Doctor of Technical Sciences, Professor, Chief Researcher  
Udmurt Federal Research Center of the Ural Branch of the RAS, Institute of Mechanics, Izhevsk, Udmurt Republic  
e-mail: [demen@udman.ru](mailto:demen@udman.ru); [kai@udman.ru](mailto:kai@udman.ru)

**Milan Vasko**, Assoc. Prof., Ing. PhD.  
University of Zilina, Faculty of Mechanical Engineering, Zilina, Slovak Republic  
e-mail: [milan.vasko@fstroj.uniza.sk](mailto:milan.vasko@fstroj.uniza.sk)

**Vladimir P. Koretskii**, PhD. in Physics and Mathematics, Senior Lecturer, MIREA, RTU, 78 Vernadsky Avenue, Moscow 119454, RF  
e-mail: [koreckij@mirea.ru](mailto:koreckij@mirea.ru)

**Pavol Bozek**, Dr.h., Prof. Ing. CSc. University of Zilina, Faculty of Mechanical Engineering, Zilina, Slovak Republic  
e-mail: [pavol.bozek@fstroj.uniza.sk](mailto:pavol.bozek@fstroj.uniza.sk)